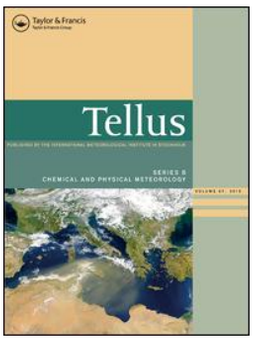

Tellus B: Chemical and Physical Meteorology

ISSN: (Print) 1600-0889 (Online) Journal homepage: http://www.tandfonline.com/loi/zelb20

Aerosol particle formation events and analysis of high growth rates observed above a subarctic wetland–forest mosaic

Birgitta Svenningsson, Almut Arneth, Sean Hayward, Thomas Holst, Andreas Massling, Erik Swietlicki, Anne Hirsikko, Heikki Junninen, Ilona Riipinen, Marko Vana, Miikka Dal Maso, Tareq Hussein & Markku Kulmala

To cite this article: Birgitta Svenningsson, Almut Arneth, Sean Hayward, Thomas Holst, Andreas Massling, Erik Swietlicki, Anne Hirsikko, Heikki Junninen, Ilona Riipinen, Marko Vana, Miikka Dal Maso, Tareq Hussein & Markku Kulmala (2008) Aerosol particle formation events and analysis of high growth rates observed above a subarctic wetland–forest mosaic, Tellus B: Chemical and Physical Meteorology, 60:3, 353-364, DOI: 10.1111/j.1600-0889.2008.00351.x

To link to this article: https://doi.org/10.1111/j.1600-0889.2008.00351.x

Tellus (2008), 60B, 353–364
Printed in Singapore. All rights reserved

TELLUS

Aerosol particle formation events and analysis of high growth rates observed above a subarctic wetland–forest mosaic

By BIRGITTA SVENNINGSSON[1]*, ALMUT ARNETH[1], SEAN HAYWARD[1], THOMAS HOLST[1], ANDREAS MASSLING[2,3], ERIK SWIETLICKI[2], ANNE HIRSIKKO[4], HEIKKI JUNNINEN[4], ILONA RIIPINEN[4], MARKO VANA[4,5], MIIKKA DAL MASO[4], TAREQ HUSSEIN[4] and MARKKU KULMALA[4], [1]*Department of Physical Geography and Ecosystems Analysis, Lund University, Sölvegatan 12, 223 62, Lund, Sweden;* [2]*Department of Physics, Division of Nuclear Physics, Lund University, Lund, Sweden;* [3]*Department of Physics, Section of Tropospheric Aerosols, Leibniz-Institute for Tropospheric Research, Leipzig, Germany;* [4]*Department of Physical Sciences, University of Helsinki, P.O. Box 64, FI-00014 University of Helsinki, Finland;* [5]*Institute of Environmental Physics, University of Tartu, Ülikooli 18, 50090 Tartu, Estonia*

(Manuscript received 25 October 2007; in final form 3 March 2008)

ABSTRACT

An analysis of particle formation (PF) events over a subarctic mire in northern Sweden was performed, based on number–size distributions of atmospheric aerosol particles (10–500 nm in diameter) and ions (0.4–40 nm in Tammet diameter). We present classification statistics for PF events from measurements covering the period July 2005–September 2006, with a break over the winter period. The PF event frequency peaked during the summer months, in contrast to other Scandinavian sites where the frequency is highest during spring and autumn. Our analysis includes calculated growth rates and estimates of concentrations and production rates of condensing vapour, deduced from the growth rates and condensational sink calculations, using AIS and SMPS data. Particle formation events with high growth rates (up to 50 nm h^{-1}) occurred repeatedly. In these cases, the newly formed nucleation mode particles were often only present for periods of a few hours. On several occasions, repeated particle formation events were observed within 1 d, with differences in onset time of a few hours. These high growth rates were only observed when the condensation sink was higher than 0.001 s^{-1}.

1. Introduction

Atmospheric aerosols have several environmental implications. Most focus is on their effects on regional and global climate (IPCC, 2007) and their adverse effects on human health (Dockery and Pope III, 1994; Pope III et al., 2002; Brook et al., 2004). In addition, aerosols are also known to have implications on, for example, acid and nutrient deposition, and atmospheric transport of toxic substances. The atmospheric aerosol influences the radiation balance in the atmosphere directly through the upward scattering of incoming short-wave solar radiation and indirectly through their capability to act as cloud condensation nuclei (CCN) and thus influence cloud microphysical properties. It has lately been suggested that the global warming can have been masked by aerosol cooling to an even higher extent than previously accounted for (Andreae et al., 2005).

We cannot fully understand the effects of anthropogenic air pollution without knowing the properties of the natural atmosphere (Andreae, 2007). The natural secondary aerosol and its changes with increasing temperature and trends in emissions of biogenic aerosol precursors have been proposed to be a vital part in feedback mechanisms of the climate, via both direct and indirect aerosol effects (Kulmala et al., 2004b). In fact, for the pre-industrial atmosphere over continental regions, secondary organic aerosol (SOA) have been arguably the chief components of cloud condensation nuclei and, even today, play a major role in that respect over large forested areas like the boreal forest and of the Amazon (Kanakidou et al., 2000; Tunved et al., 2006;

*Corresponding author.
e-mail: birgitta.svenningsson@nuclear.lu.se
DOI: 10.1111/j.1600-0889.2008.00351.x

Andreae, 2007). Changes in emissions of biogenic precursors and their interactions with aerosol particle formation and growth are important processes that needs to be understood in that context.

New particle formation in the atmosphere has been observed all over the globe (Kulmala et al., 2004c), in clean background air masses as well as in polluted air. It is most often observed during daytime, indicating that photochemical reactions in the atmosphere probably are of importance as well as the mixing taking place when the boundary layer breaks up (Nilsson et al., 2001). Only very few observations of night time events are described in the literature (Suni et al., 2007). The effect of new particle formation in the boundary layer on the aerosol particle concentrations on a global scale has been studied using a global aerosol microphysics model (Spracklen et al., 2006). Their results suggest that particle concentrations at remote areas are dominated by secondary particles, whereas in polluted areas, the primary particles are most important for the particle number concentration. They also showed that the atmosphere responds in a complicated way to changes in emissions. As an example, reductions in primary particle emissions can increase the particle number concentration due to the decreased quenching of particle formation.

The chemical composition of the newly formed aerosol particles is in general not known, even though sulphuric acid probably plays a key role in the very initial stage (Weber et al., 1996; Sihto et al., 2006; Riipinen et al., 2007) and iodine compounds have been identified in coastal particle formation (O'Dowd et al., 2002, 2004). There is also some evidence for biogenic monoterpene emissions playing an important role in particle formation in at least eucalyptus and boreal forests (Kavouras et al., 1998; Tunved et al., 2006). Di-methyl amine in the particle phase has also been associated with particle formation events (Mäkelä et al., 2001). Nevertheless, we still do not know the chemical substances that are responsible for the onset of particle formation or the compounds that make the newly formed particles grow into detectable sizes and further to sizes where they can act as cloud condensation nuclei.

Chemistry aside, in terms of the microphysics of particle formation, mechanisms for the nucleation and early growth of atmospheric aerosol particles have been discussed and one of the recent models (Kulmala et al., 2000; Kulmala, 2003; Kulmala et al., 2004a) assumes that thermodynamically stable clusters of about 1 nm in diameter or less exist all the time in the atmosphere. It is assumed that they can become activated by supersaturated vapours of, for example, organic compounds and then start to grow. Charged clusters are always present, and some experimental and theoretical support for the existence of neutral clusters have been presented (Kulmala et al., 2005a, 2007).

Most of the data concerning particle formation in northern locations are from boreal forests with comparatively little direct human pollution influence (Kulmala et al., 2004c; Dal Maso et al., 2007). There is evidence pointing at biogenic emissions from boreal forests as important precursors for the evolution of the natural atmospheric aerosol over northern Scandinavia (Tunved et al., 2006). However, typical northern latitude ecosystems like wetlands or tundra generally have been ignored as major SOA precursor areas, although it is known that these emit isoprene as well as monoterpenes at measurable amounts (Hakola et al., 1998; Janson and De Serves, 1998; Hellén et al., 2005). This is particularly important, since isoprene has been discovered to contribute to SOA growth, and since global climate change may lead to tree-line migration and a different relative contribution of forest versus wetland versus tundra ecosystems in northern landscapes (Chapin et al., 2004; Claeys et al., 2004). Whether or not such a change in vegetation will have effect on aerosol particle formation or concentration is unkown.

In this work, we have analysed aerosol particle and air ion size distributions taken at a subarctic site in northern Sweden and characterized events of new particle formation. Also, night time events with high growth rates are presented and analysed. The condensation sink of the submicrometre aerosol has been estimated and growth rates calculated for the particle formation events. Ambient concentrations and production rates of condensable vapours are estimated. The influence of condensation sink on particle event characteristics is investigated. However, detailed analysis of meteorological conditions, back trajectories and behaviour of cluster ions will be the subject of future studies and is not included here.

2. Experimental

2.1. Site

Measurements were conducted at Stordalen mire (68.35°N, 19.05°E), approximately 14 km east of Abisko; a subarctic mire underlained by discontinuous permafrost (Fig. 1). The larger Abisko area is characterized by subarctic birch forest (Betula pubescens) interspersed with wetlands and, above the tree line, tundra ecosystems. Long term average mean temperature at the site (1913–2002) were −0.7°C, with considerable fluctuations over this period, particularly two warming periods: one in the early half of the 20th century, the other over recent decades (Christensen et al., 2004). Monitoring of vegetation patterns on the mire in the 1970s allowed to assess rapid changes in surface hydrology and vegetation patterns in response to this latter warming (Svensson et al., 1999), which fosters expansion of wetter parts of the mire dominated by sedges over the drier parts of the mire, formed by Sphagnum and ericaceous shrubs.

2.2. Instrumentation

Precise particle number–size distribution measurements in the submicrometre size range are generally based on particle mobility techniques, for example, the application of scanning mobility particle sizers (SMPS). As a first step, the aerosol is given a well-defined charge distribution in a neutralizer, and the

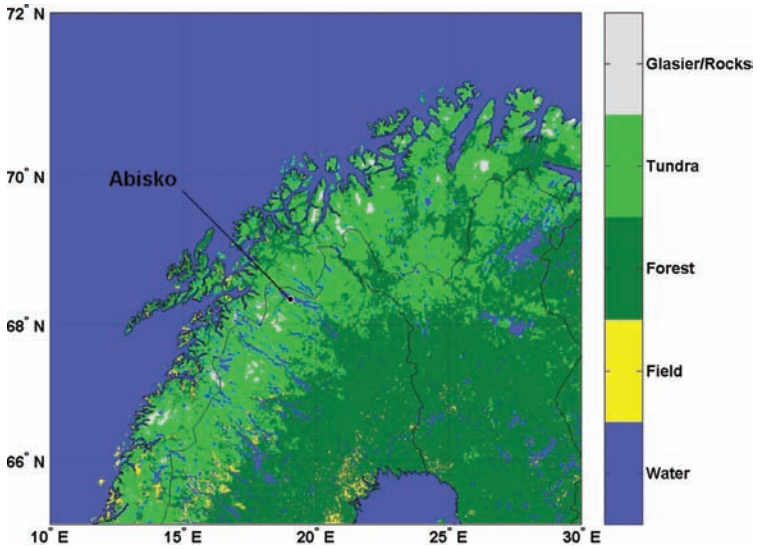

Fig. 1. A map over northern Scandinavia, with vegetation zones indicated (courtesy of the U.S. Geological Survey, http://www.usgs.gov). The Abisko region is characterized by birch forests, mires and lakes and is surrounded by mountains. The measurement site is situated on the Stordalen mire, 14 km east of Abisko.

electrically charged particles are classified according to their electrical mobility in a differential mobility analyzer (DMA). As a result, particles within a narrow size range leave the DMA and the number concentration of these particles is counted by a condensation particle counter (CPC) in different mobility classes (Birmili et al., 1999).

In this study, we used a custom built SMPS continuously scanning the size range between 10 and 500 nm with a time resolution of 3–5 min (DMA: Hauke type medium, custom built; CPC: 3010, TSI Inc., USA). An exact measurement of the real particle number–size distributions requires high demands on the calibration of the individual parts of the measurement device. As a part of the data quality control, closed loop (sheath/excess air) and sample air flow rates, as well as their temperatures, relative humidities and the inlet pressure were monitored continuously during the whole measurement period. In addition, diffusion dryers within the sheath/excess air cycle were used. The SMPS was first placed in a trailer on the mire, with the inlet 3.4 m above the ground and flow rate in the inlet tubing of 17 $l\,min^{-1}$. In May 2006 it was moved to a small house next to the mire and a birch forest, and the length of the inlet tubing was increased to 4.4 m. Using an inversion algorithm, real particle number–size distributions were calculated, based on the determined raw particle mobility distributions, taking into account diffusion losses in the sample lines, probability for multiple charging, DMA transfer function including diffusion losses in the DMA and CPC efficiency.

The early stage of particle formation has only recently been accessed (Kulmala et al., 2007), and the detection of the smallest neutral particles is still very challenging and needs more investigation. One of the possibilities to study these early stages, the air ion spectrometer (AIS #5, manufactured by Airel Ltd., Estonia; Mirme et al., 2007), is used in this study. In a similar principle to DMA techniques, the AIS measurement is based on the mobility of charged clusters and particles in an electric field. Since there is no charger at the inlet in the AIS, only naturally charged clusters and particles are detected. The sample flow is introduced close to the central electrode and the charged entities move towards the outer electrode that consists of 21 segments, each of them attached to an electrometer. Two columns, one for the negative and one for the positive ions and clusters, are used. The whole mobility distribution is thus obtained simultaneously, with a time resolution of 5 min, and no scanning is needed. The AIS gives air ion mobility spectra for the mobility range 3.2–0.0013 $cm^2\,V^{-1}\,s^{-1}$, corresponding to a diameter range of 0.4–40 nm (Tammet, 1995). More details about the instrument, its performance and the data processing are given by Mirme et al. (2007). The AIS has short inlet tubing and samples at a height of about 1.7 m above the ground. Our instrument was calibrated versus a BSMA (Tammet, 2006) to account for losses of small ions.

Meteorological data for the site is available from a meteorological mast run by the University of Copenhagen. The mast is located in the centre of the mire, about 10 m from the trailer, and it includes measurements of net radiation, incoming shortwave radiation, air temperatures and humidity, soil temperatures and precipitation. Data for air temperature and humidity used in the condensational sink calculations (*CS*, Section 2.3) was measured by a combined Pt-100 temperature and capacitive humidity probe (Rotronic MP103A, Crawley, UK) at a height of 2.4 m above ground level. The accuracy of this sensor type is about 0.3 K for temperature and 1.5% RH for humidity. All sensors are sampled automatically using a CR10X datalogger (Campbell Scientific, Logan, USA) and recorded as hourly mean values or totals, respectively.

2.3. Data evaluation

The particle formation events observed using the SMPS (10–500 nm) were classified according to the scheme proposed by

Dal Maso et al. (2005). Generally, for a day to be classified as a particle formation day, there should be a new particle mode appearing in the diameter range below 25 nm, and this new mode should grow in size and persist for more than 1 h. In contrast, non-event days are characterized by the absence of new mode of sub-25 nm particles that exists for more than 1 h and no growing Aitken mode. Days that do not follow any of these two specifications are labelled unclassified.

The classification of the air ion size spectra is more complicated, and a common classification scheme is still under development. Air ion spectra (AIS) frequently show outbreaks of intermediate ions (1.6–7 nm in diameter), caused by a variety of processes, many of them unknown. The full classification under development will take all of them into account. In this work, a simplified classification was applied for the purpose of analysing particle formation. This classification is based on the classification of SMPS data described above, with the size range for the new mode specified as 1–10 nm and the minimum limit for growth set to diameters above 10 nm. Using such an approach, for a subset of the event days, the diameter growth rate of the newly formed particles could be determined (equivalent to class I events according to Dal Maso et al., 2005). In class II events, there was too much variability in particle concentration for the growth to be characterized.

Traditionally, classification of aerosol particle formation is made on a day-by-day basis. This is justified by most events appearing during day time, and most often, only one event per day is observed. In the data presented here, many events were observed during the night and there was often more than one outbreak of new particles/ions per day. Furthermore, in the air ion size spectra, several different types of events can take place during 1 d. For the future, it should be considered finding a classification method taking into account these processes. However, in this paper, we follow the tradition and classify the events day-by-day. In the analysis of growth rates as a function of, for example, condensation sink or time of day and year, more than one event per day, when present, was included.

The aerosol particle number–size distribution (SMPS) data were fitted to up to three lognormal distributions (Hussein et al., 2005). A similar approach was used to fit lognormal distributions to the air ion size spectra. This generated two modes for both, negative and positive ions. One of the fitted lognormal modes was forced to always fit the cluster ion mode ($<$1.3 nm).

The evolution of the modal diameter with time was used to find the growth rate of the particles by fitting a line to particle diameter as a function of time, the slope of which is interpreted as the growth rate. In this methodology, it is assumed that the particle formation takes place in a homogeneous air mass and that the particles observed during the modal diameter growth are all formed at the same time. For the AIS data, priority was put to the growth of the newly formed particles in the size range 1–10 nm although especially the events with high growth rates often showed the same growth rate in the whole range up to 40 nm. For the SMPS data, the growth rate was determined as an average over the time when the new mode was observed. For events with long duration, only the growth until midnight of the first day was taken into account.

The growth rate depends on the concentration of condensable vapours (Kulmala et al., 2005b). Assuming that the ambient vapour pressure is much higher than the saturation vapour pressure over the particle surface and properties similar to those of sulphuric acid, the growth rate (GR in nm h^{-1}) for particles in the transition regime (for our purpose those larger than 5 nm in diameter) can be expressed by a linear relation to the concentration of condensable vapours (C in cm^{-3}) (Kulmala et al., 2001):

$$GR = 1.39 \times 10^7 \times C \tag{1}$$

The condensation sink parameter (CS) describes the timescale ($1/CS$) for removal of condensable vapours due to condensation on pre-existing particles. It is calculated from the aerosol particle size distribution, assuming that the saturation vapour pressure over the particle surface is low compared with the vapour pressure far from the particle and molecular properties similar to those of sulphuric acid:

$$CS = 2\pi D \sum_i \beta_i d_{pi} N_i . \tag{2}$$

where D is the diffusion coefficient for the condensing vapour, d_{pi} is the diameter of particles in class i, N_i is their number concentration and β_i is the transitional correction factor. The condensation sink depends on the ambient size of the particles, including the liquid water. As we do not have information about the hygroscopic growth of the particles during this experiment, we estimated the water uptake of the observed aerosol based on measurements at the boreal forest site in Hyytiälä, Finland and applied the hygroscopicity parameterisation by Laakso et al. (2004).

The time dependence of the concentration of condensable vapours (C) can be expressed as:

$$\frac{\mathrm{d}C}{\mathrm{d}t} = Q - CS \times C, \tag{3}$$

where Q is the vapour production rate. For the purpose of order-of-magnitude estimations of vapour production rates, we assume steady state conditions ($\mathrm{d}C/\mathrm{d}t = 0$). The vapour concentration is then determined by the production rate and the condensation sink as

$$C = Q/CS \tag{4}$$

On the other hand, if we know C, the vapour production rate can be estimated as:

$$Q = CS \times C. \tag{5}$$

More details concerning these calculations are given by Kulmala et al. (2001, 2005b).

3. Results and discussion

3.1. Aerosol and cluster ion characterization

The air in the Abisko region is most of the time relatively unpolluted background air of arctic origin that has been transported over land with low population density for time periods of hours to days. The site can, on some days, be influenced by air from more polluted areas in, for example, southern Scandinavia and central Europe. Accordingly, the number concentration of particles in the size range 10–500 nm (SMPS) varied from less than a hundred to a couple of thousand particles per cubic centimetre, with an average over the measurement period of 790 cm^{-3}. The time-series of daily and monthly averages (Fig. 2a) shows slightly higher particle number concentrations during summer compared with spring and autumn.

Variation in aerosol particle size distribution data can be illustrated using many different parameters, for example, total number, surface, volume or modal structure. For the purpose of understanding particle formation and concentrations of clusters and condensable vapours, the condensation sink (*CS*, see Section 2.3 and Kulmala et al., 2005b) is a valuable measure. At our Stordalen site, the average *CS* during the measurement period was 0.0025 s^{-1}, indicating a life time of condensable gas molecules of 5–10 min, if no other sinks are assumed. Daily averages of *CS* as low as 0.00025 s^{-1} were observed (Fig. 2b). The average *CS* in Abisko is comparable to the *CS* at background sites in central Finland (Dal Maso et al., 2007) and clean conditions in Southern Sweden (Kristensson et al., 2008).

In the air ion spectra, the typical picture of an always present mode of cluster ions with modal diameters in the range 0.5–1 nm (diameter according to Tammet, 1995) is clearly visible (Figs. 3e–h). The negative ions were in general smaller (with an average diameter of 0.65 nm) compared with the positive ones (0.82 nm), but they also show more variability in size. Cluster ion number concentration are presented in Fig. 2(c), and the numbers of negative and positive cluster ions (based on the fitting) averaged 2380 cm^{-3} and 1650 cm^{-3}, respectively. These cluster ion concentrations are higher than observed at many other sites (Komppula et al., 2007; Vartiainen et al., 2007; Venzac et al., 2007). However, the overall picture of an always present cluster ion mode agrees with the previous observations.

The ion concentration in the size range 1.6–7 nm (intermediate ions) is normally low, with various types of outbreaks of higher concentration having durations of a few minutes to hours. Several processes are responsible for these outbreaks, many of them not very well known. For the analysis of the AIS data, we focus here on particle formation events, that is, occurrence of intermediate ions that showed growth leading to formation of particles larger than 10 nm in diameter.

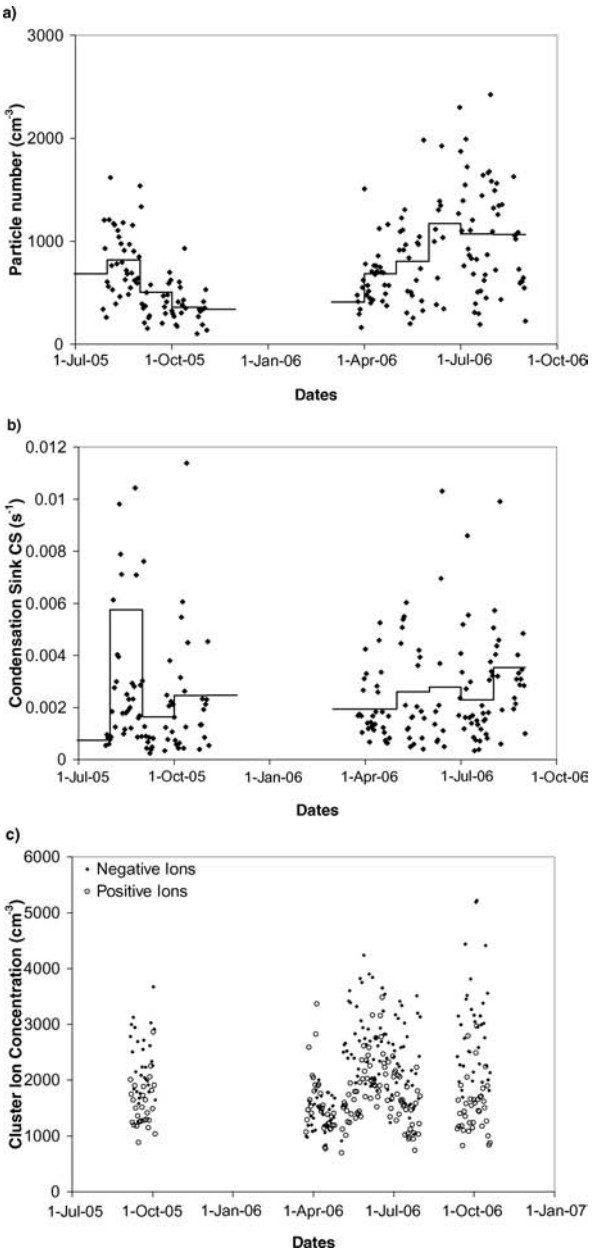

Fig. 2. Daily and monthly averages of (a) number concentration of particles in the size range 10–500 nm in diameter and (b) condensation sink (*CS*) estimated from the aerosol particle size distributions (SMPS data). (c) Daily averages of negative and positive cluster ions according to the fit of a lognormal distribution with a modal diameter smaller than 1.3 nm to the size distributions of the naturally charged particles in the diameter range 0.4–40 nm (AIS data). The grand average for the negative and positive cluster ion concentrations are 2380 and 1650 cm^{-3}, respectively.

3.2. Particle formation events

Particle formation, according to the classification described in Section 2.3, was frequently observed. It should be noted that the time periods covered by AIS and SMPS differed due to different starting dates and instrument failures. The determined growth rates and times of onset can also be different since the two sets of data cover different size ranges, and the focus in the AIS data

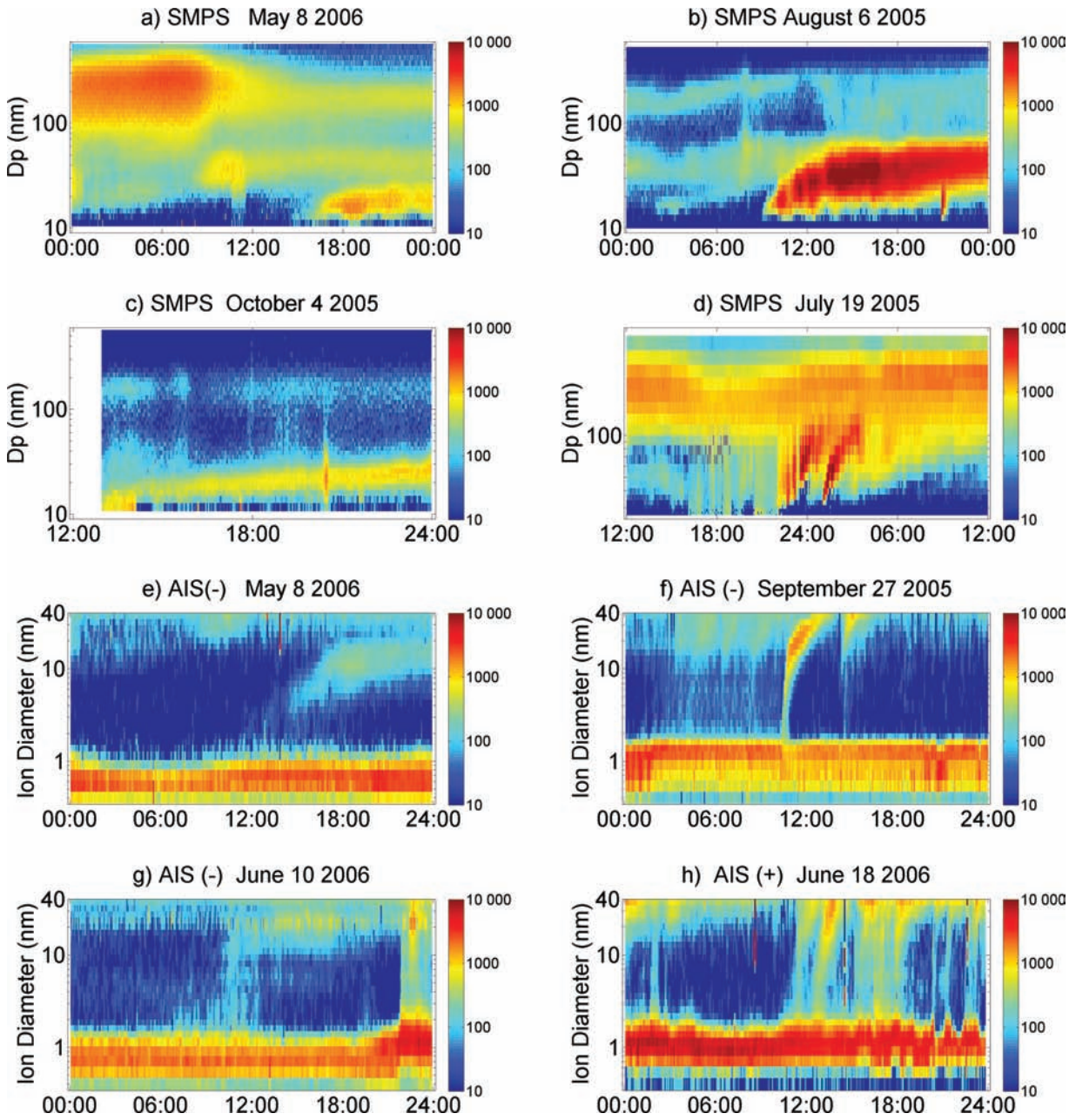

Fig. 3. Time evolution of aerosol particle (a–d) and ion (e–h) size distributions. The *x*-axis represents time, *y*-axis particle/ion size, and the colour code the number concentration (dN/d logDp, cm^{-3}). (a) A typical particle formation event. The formation and growth of negatively charged ions during the same event is shown in panel (e). (b) Strong formation event in an air mass coming from the Barents Sea. (c) Particle formation event in a very clean air mass with origin over the Norwegian Sea. (d) Two consecutive nighttime events with high growth rates. (e) A typical particle formation event as seen in the growth of negative ions. The growth of aerosol particles (neutral and charged) during the same event is shown in Fig. 3a. (f) High growth rates of the negative ions. The positive ones showed a similar picture. (g) Nighttime event with high growth rate and an increase in cluster ion size at the same time. (h) This is an example where the cluster ion size is strongly affected and particle formation is trigged several times—during some of these particle bursts, the growth was too high to be determined.

analysis is on the growth of particles below 10 nm in diameter, a size range not covered by the SMPS data. In the range of overlapping sizes (10–40 nm in diameter), the data from the two instruments show, in general, a consistent picture of the ion/particle size distributions (Figs. 3a and e). In a few cases, however, there are clear discrepancies, and some of these will be discussed below. In the following, we will first give three examples of particle formation events observed in the SMPS data (Figs. 3b–d), along with some of their characteristics. After that, we will give example from the

AIS data and make some comparison between the two sets of data.

According to the classification of the SMPS data, 77 out of 195 d (40%) were particle formation event days. The data on which these numbers are based cover spring, summer and autumn but not winter. 60% of the particle formation events that were seen in the SMPS data, took place during daytime and showed moderate growth rates (0.5–10 nm h^{-1}, Figs. 3a–c), an observation in agreement with observations from other continental background sites (Kulmala et al., 2005b). As a typical pattern observed for summer time conditions, during the particle formation event on 6 August 2005 (Fig. 3b), the air mass originated from the Barents Sea and arrived from north after travelling over land for about 12 h (according to HYSPLIT back trajectories, http://www.arl.noaa.gov/ready.html; Draxler and Rolph, 2003; Rolph, 2003). On that day, the morning concentration of particles in the size range 10–500 nm was just below 200 cm^{-3}. The number of particles in the newly formed mode reached a maximum of 3500 cm^{-3} at 15:00, 6 h after it first could be detected in the SMPS data. At 20:00, there were still 2000 particles cm^{-3} with a modal diameter of 37 nm (Fig. 3b). The calculated growth rate was 4.5 nm h^{-1}, corresponding to a concentration of condensable vapours of 6×10^7 cm^{-3} and a vapour production rate of 1×10^5 cm^{-3} s^{-1}. The new particle mode was observed for in total almost 2 d and after 1 d, the modal diameter was 65 nm. Depending on the particle chemical composition and cloud formation dynamics, particles of this size can act as cloud condensation nuclei. This is an example of how the aerosol particle size distribution can be strongly affected by particle formation in the atmosphere during seasons with high biological activity.

A second example is taken from the autumn measurement period, when vegetation on the mire is not active anymore and leaf fall at the birch forest had commenced (4 October 2005 SMPS aerosol particle size distributions in Fig. 3c). In this case, the air mass originated from the Norwegian Sea and arrived in the Abisko area from western directions after less than 6 h passage over land. During the first hour of this event, the concentration of particles larger than 15 nm was 70 cm^{-3}; there is unfortunately no size distribution data available before the onset of this event. At midnight, the modal diameter of the new particle mode had reached 25 nm and the number concentration was 310 cm^{-3} (compared with a total of 340 particles cm^{-3} in the particle diameter range 10–500 nm). The calculated growth rate was 0.9 nm h^{-1} (Fig. 3c), corresponding to a concentration of condensable vapours of 1×10^7 cm^{-3} and a vapour production rate of 3×10^3 cm^{-3} s^{-1}. Here it is shown that for this type of clean conditions, low production rates of condensable vapours, also, can alter the aerosol particle size distribution significantly.

In addition to this type of often described daytime events, we frequently observed events that did not fit into this pattern (see e.g. Fig. 3d). They were characterized by unusually high growth rates, estimated under the assumption of a homogeneous air mass and were of relatively short duration (i.e. few hours). In many of these events, the onset took place during the night (Fig. 4a) and they were often, though not exclusively, observed in summer. In the Abisko area, the sun is above the horizon all night from 31 May to 14 July, although the sun light is not very intense during the night. In many cases, repeated particle bursts were possible with time intervals between each burst of typically a few hours. In the SMPS data, we observed growth from 10–30 nm up to 100 nm taking place within a few hours (Fig. 3d). If these particles consist of soluble material with molar weights similar to those of oxidation products of monoterpenes, they are expected to be good cloud condensation nuclei.

According to the AIS data classification, 44 out of 175 d (26%) showed particle formation, covering both high and low growth rates (see for example Fig. 3e) and onset during the day as well as during the night (Fig. 4b).

Particle formation events with high growth rates, and sometimes nighttime onset, are observed in the AIS data as well. Events were observed with growth from cluster ion size to the upper diameter limit of the instrument (40 nm) taking place in 1–2 h (Figs. 3f–h). The highest growth-rate determine from the AIS data was 57 nm h^{-1}, which is a conservative estimate because, in some cases, the instrumental time resolution limited the possibility to judge between growth and ions of all sizes appearing simultaneously (Fig. 3h). Many of the high growth rate events were associated with an increase in the cluster ion sizes, examples of which are presented in Figs. 3(g)–(h). In these cases, negative and positive cluster ions typically ended up at similar sizes although the change is most pronounced for the negative ones, since they started from smaller sizes.

Figure 3(f) shows an example of AIS data from one day in a week in September 2005, with 5 of 7 d showing this type of strong particle formation. One very clear event for which the growth rate easily could be determined, is illustrated in the figure. Several less clear bursts of intermediate and larger ions are observed before and after that. During this period, a particle formation event with high growth rates and onset after the sunset was observed. However, the events during this week did not appear as pronounced in the SMPS data. During this period, the SMPS was placed in the trailer on the mire and the AIS was located in a house at the border of a birch forest next to the mire. The distance between the instruments ($\sim$300 m) and their different immediate environments could be a clue to the differences found here and is a motive for further investigations.

At this point, we cannot draw conclusions on the reason for high growth rates and onset of particle formation during the night. It is, however, not very likely that photochemical reactions or boundary layer break up are the driving force behind these night time events.

3.3. Seasonality of particle formation events

The seasonality of particle formation events is illustrated in Fig. 5 (5a based on SMPS and 5b on AIS data). Data from both

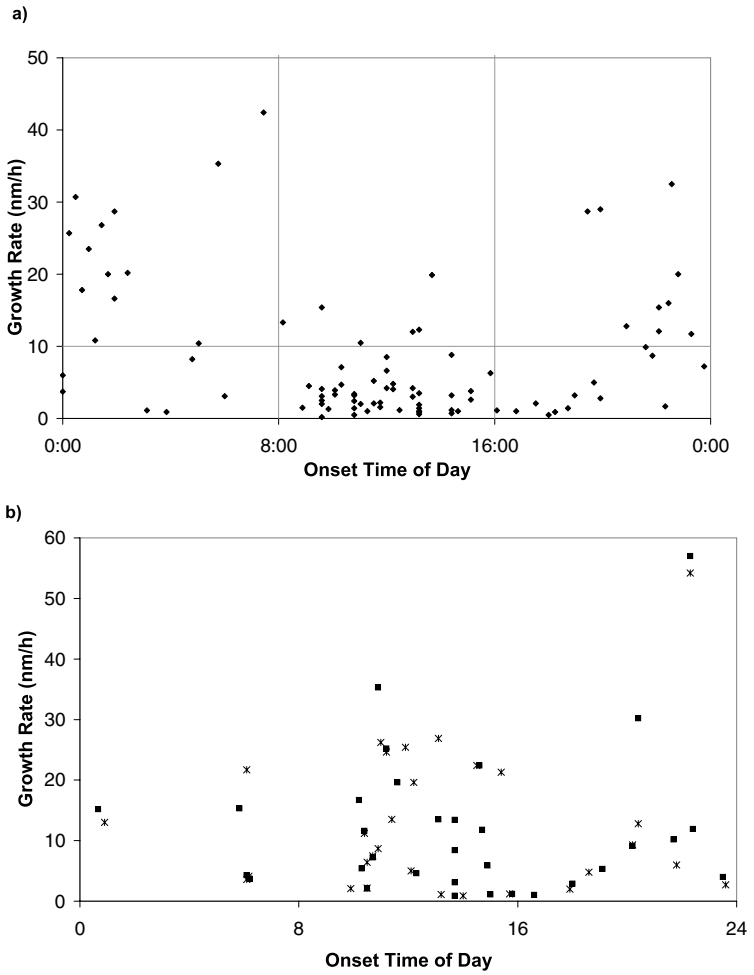

Fig. 4. Growth rate as a function of the time of the day when the new mode was first observed in (a) SMPS and (b) AIS data. The solid lines in (a) represent the division between the nighttime events with high growth rate (onset between 16:00 and 8:00 and growth rates higher than 10 nm h^{-1}) and the rest of the events.

instruments show a maximum in the frequency of particle formation events during the summer. The SMPS data gave, in general, somewhat higher particle formation frequencies, compared with the AIS. A period of very high particle formation frequency in June 2006 found in the SMPS data is, however, based on 12 d only. The summer maximum contrasts observations from sites in southern Scandinavia (Dal Maso et al., 2007; Kristensson et al., 2008; Hyvärinen et al., 2008) where particle formation events were concentrated in the spring and autumn months. The sites in northern Finland, at about the same latitude as Stordalen, show less pronounced spring and autumn maxima. The spring onset at these sites is, however, earlier than in Stordalen, and they do not show a summer peak in the particle formation event frequency (Dal Maso et al., 2007).

The particle growth rate (Fig. 6) is a function of the condensable vapour concentration, which in itself is a function of the vapour production rate (Q) and the condensation sink. Like the growth rates, also the vapour production rates, estimated from growth rates and the condensation sink, peaked during summer. The summer maxima in the growth rate and Q is in agreement with previous observations (Kulmala et al., 2005b; Dal Maso et al., 2007; Kristensson et al., 2008) and consistent with the biological activity and emissions of photosynthesis related aerosol precursors (e.g. isoprene and monoterpenes) being high in the summer. We did, however, find high growth rates, and thus high values of Q also, in late September (see e.g. Fig. 3f), when the photosynthesis and emissions of related biogenic aerosol precursor vapours were low. One hypothesis is that the decay of biological material can result in aerosol precursors. Mäkelä et al. (2001) has, for example, observed that the concentration of di-methyl amine in aerosol particles was higher during event days compared with non-event days. Di-methyl amine is an end product of microbial decomposition of organic material and the observations could thus possibly be linked to freshly fallen birch litter.

3.4. Particle formation event days versus non-event days

Differences in particle number (in the size range 10–500 nm) and *CS* for particle formation event days compared with non-event days were investigated. We divided the particle formation events into two groups: (1) particle formation events with growth

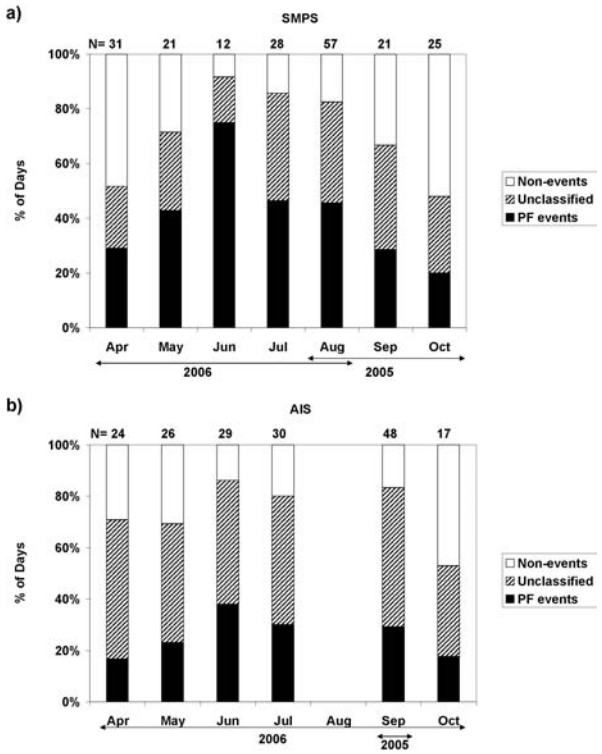

Fig. 5. Seasonality of days with particle formation events from (a) the SMPS and (b) the AIS. *N* represents the number of days with valuable data during each month. Black bars, particle formation event days; white bars, non-event days and striped bars, unclassified days.

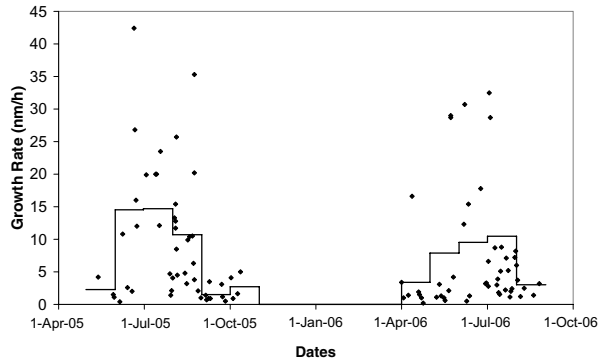

Fig. 6. Daily and monthly averages of growth rates as determined from the SMPS data.

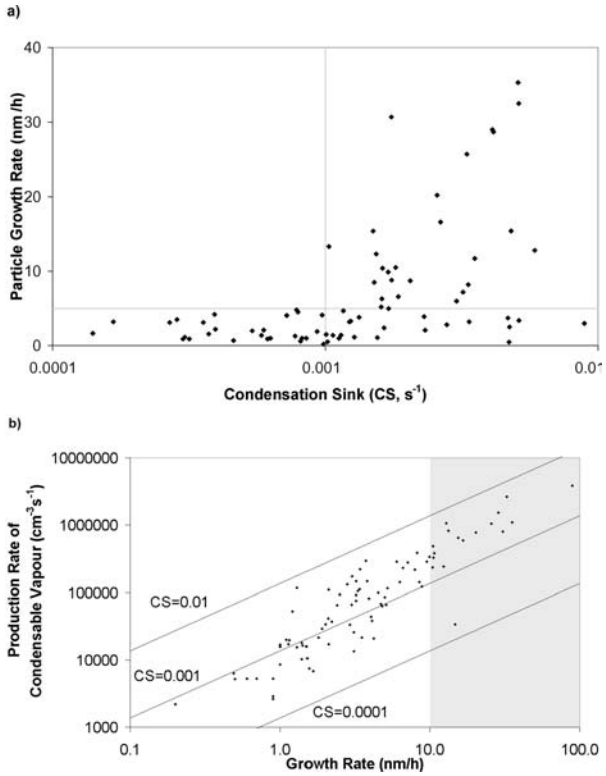

Fig. 7. (a) The particle growth rate determined from the SMPS data versus the condensation sink averaged over half an hour before the new mode was first observed. (b) The estimated production rate of condensable vapour (Q) versus the particle growth rate. The solid lines represent the vapour production rate that can sustain a given particle growth rate for three values of the condensation sink (CS): 1×10^{-2} s^{-1}, 1×10^{-3} s^{-1}, and 1×10^{-4} s^{-1}. The high Q values, associated with growth rates over 10 nm h^{-1}, should be taken with precaution as discussed in Section 3.4.

rates over 10 nm h and onset during the night (upper left- and right-hand side areas in Fig. 4a) and (2) all other events. We found that the particle number was in average higher during event days with high growth rates and onset during nighttime (average $\pm$ 1SD = 1070 $\pm$ 342 cm^{-3}) compared with the other event days (782 $\pm$ 451 cm^{-3}) and non-event days (666 $\pm$ 481 cm^{-3}).

Comparing the average values for the condensation sink in the same way, we found no difference between the high growth-rate events (0.0032 + 0.0014 s^{-1}) and non-events 0.0031 + 0.0024 s^{-1}). The other events showed, in average, lower values of CS (0.0017 $\pm$ 0.0015 s^{-1}). In previous studies, it has been observed that the particle formation events often are associated with lower values of the condensation sink (and thus also lower coagulation sink) compared with non-event days (Dal Maso et al., 2007). This can be explained by less competition for condensable vapour when CS is low (eqs. 3 and 4) and a longer lifetime of the newly formed particles and hence a higher probability for newly formed particles to grow to detectable sizes.

Figure 7a shows the growth rates as a function of the condensation sink, averaged over half an hour before the new mode was first observed in the SMPS data. From eqs. (1) and (4), the growth rate is expected to correlate with the inverse of the condensation sink. But Fig. 7(a) shows the opposite—the high growth rates were only observed when the condensation sink was above 1×10^{-3} s^{-1}. We investigated this further by plotting the vapour production rate (Q estimated as described in Section 2.3) versus

the growth rate (Fig. 7b), which showed a similar picture—high growth rates were associated with high Q. Some important assumptions are made in the estimates of Q: the particle growth is assumed to take place in a homogenous air mass and the vapour concentration is assumed to be in steady-state. Even though the particle formation events with the highest determined growth rates continued for time periods of at least five times the typical life times of condensable vapours, we cannot exclude that these assumptions are violated during some of these events. Q associated with growth rates over 10 nm h^{-1} (the shaded area in Fig. 7b) should therefore be taken with precaution. The solid lines in the Fig. 7(b) represent the values of Q needed to sustain a given growth rate for three different values of CS: 1×10^{-2}, 1×10^{-3} and 1×10^{-4} s^{-1}. The Q values needed to explain the observed growth rates increases even stronger than indicated by these lines, which is consistent with the high growth rates being associated with relatively high CS . Thus, the condensation sink cannot explain the high growth rates and their explanation should be sought for elsewhere.

The event-quenching ability of a high coagulation sinks (related to the condensation sink) can, in some cases, explain correlations between condensation sink and particle growth rate. If the coagulation sink is high, newly formed particles will be quickly scavenged by the pre-existing particles, and no particle formation event is observed unless the growth rate is high. Because of the competition between growth and scavenging, the only types of events observed are the ones with either extremely high formation rates or high growth rates. This explanation, however, suggests that the high growth rates are observed at all CS and a lack of low growth rates at high CS. It cannot give a reason for the high growth rates not being observed during periods with low condensation sink.

The association of high growth rates with higher than average particle number concentrations, could be the results of the particle formation increasing the particle number or an effect of the high growth rate events taking place in air masses that are more polluted, or where atmospheric particle formation has taken place already upwind of Stordalen. But, the fact that the condensation sink prior to events with high growth rates were higher than those found before the onset of the other events, suggests that the former took place in air masses with higher concentrations of pre-existing aerosol particles.

The reason for the coexistence of the high growth rates and the larger CS values cannot be explained by aerosol and vapour dynamics only, as already discussed. It suggests that either the particles contributing to the CS and the aerosol precursors came from the same sources (natural or anthropogenic) or that their sources are located in the same wind direction or along the same set of back-trajectories. Alternatively, there could be a synergistic effect between local biogenic precursor emissions and long distance transported trace gases, coming from the same sources as the particles contributing to the condensation sink. Furthermore, due to the short duration of these events and the fact that they have not been observed at other sites, we cannot exclude that they were caused by local phenomena or mixing processes. At this stage, no conclusions on why these high growth rates appear at this subarctic site can be drawn, and further analyses taking various processes into account are needed.

4. Conclusions

The presented data show a unique study of particle formation processes as measurements were conducted at a remote site with low impact of anthropogenic influence. Size distributions of atmospheric aerosol particles (10–500 nm) and naturally charged particles and cluster ions (0.4–40 nm) at this background site in northern Sweden have been analysed. The averages of particle number concentration and condensation sink were 790 cm^{-3} and 0.0025 s^{-1}, respectively. The slightly higher particle number concentrations during the summer compared with spring and autumn is consistent with the higher emissions of biogenic aerosol precursors related to photosynthesis during this period.

Particle formation is a frequent phenomenon even at this subarctic site. It influences the aerosol particle size distribution strongly, especially when it takes place in clean air of marine origin. Particle formation events in which the newly formed particle mode reaches a size where the particles can act as cloud condensation nuclei are observed. Also, very low vapour production rates (3×10^3 cm^{-3} s^{-1}) can sustain a particle growth that significantly changes the aerosol particle size distribution under these clean conditions.

The particle formation event frequency peaks in the summer (June–August), which is in contrast to measurements in boreal forests. The growth rates of the newly formed particles are also highest in the summer, which is in agreement with many other observations.

The condensation sink is, in general, lower at days with particle formation compared with non-event days. This is expected from the longer life-times of newly formed particles and higher probability for them to grow to detectable sizes in the case of a low coagulation (and condensation) sink. A similar behaviour has been found also at other sites.

A type of particle formation events, not previously observed, is often seen at Stordalen. These events are characterized by high growth rates (up to about 50 nm h^{-1}), often nighttime onset, durations of a few hours, and often 2 or more particle bursts after each other. Growth rates this high have only been observed at a few sites, preferentially during coastal particle formation events. Frequently, the particle diameter was close to 100 nm in the end of this type of particle bursts. Particles of this size are expected to be able to act as cloud condensation nuclei.

High growth rates (>5 nm h^{-1}) are only observed when the condensation sink is higher than 1×10^{-3} s^{-1}, with an average of 3.2×10^{-3} s^{-1}. This value is similar to that found for non-event days and higher than the average for other events. Possible reasons for the high growth rates and their coexistence with

relatively high condensation sinks are discussed—the condensation sink being connected to the same source as the condensing vapour source or being found along the same trajectory, or a synergistic effect between locally emitted precursors and long range transported compounds. However, local phenomena and mixing processes cannot be excluded as reasons for apparently high growth rates. At this stage, no conclusions on the reason for the high growth rates observed at this subarctic site can be drawn, and further investigations of this phenomenon is strongly recommended.

5. Acknowledgments

This work is supported by the European Commission via a Marie Curie Excellence Team Grant and by the Swedish Research Council. M. Dal Maso wishes to thank the Maj and Tor Nessling foundation for financial support. We would also like to acknowledge the support from BACCI Nordic Centre of Excellence and Abisko Scientific Research Station. The authors gratefully acknowledge the NOAA Air Resources Laboratory (ARL) for the provision of the HYSPLIT transport and dispersion model and READY website (http://www.arl.noaa.gov/ready.html) used in this publication. In addition, we want to thank Thomas Friborg for letting us use his temperature and relative humidity data.

References

Andreae, M. O., Jones, C. D. and Cox, P. M. 2005. Strong present-day aerosol cooling implies a hot future. *Nature* **435**, 1187–1190, doi:1110.1038/nature03671.

Andreae, M. O. 2007. Aerosols before pollution. *Science* **315**, 51–52.

Birmili, W., Stratmann, F. and Wiedensohler, A. 1999. Design of a DMA-based size spectrometer for a large particle size range and stable operation. *J. Aerosol Sci.* **30**, 549–553.

Brook, R. D., Franklin, B., Cascio, W., Hong, Y. L., Howard, G. and co-authors. 2004. Air pollution and cardiovascular disease – a statement for healthcare professionals from the expert panel on population and prevention science of the American Heart Association. *Circulation* **109**, 2655–2671.

Chapin, F. S., III, Callaghan, T. V., Bergeron, Y., Fukuda, M., Johnstone, J. F. and co-authors. 2004. Global change and the boreal forest: thresholds, shifting states or gradual change? *AMBIO, J. Human Environ.* **33**, 361–365.

Christensen, T. R., Johansson, T., Åkerman, H. J. and Mastepanov, M. 2004. Thawing sub-arctic permafrost: effects on vegetation and methane emissions. *Geophys. Res. Lett.* **31**, doi:10.1029/2003GJ018680.

Claeys, M., Graham, B., Vas, G., Wang, W., Vermeylen, R. and co-authors. 2004. Formation of secondary organic aerosols through photooxidation of isoprene. *Science* **303**, 1173–1176.

Dal Maso, M., Kulmala, M., Riipinen, I., Wagner, R., Hussein, T. and co-authors. 2005. Formation and growth of fresh atmospheric aerosols: eight years of aerosol size distribution data from SMEAR II, Hyytiala, Finland. *Boreal Environ. Res.* **10**, 323–336.

Dal Maso, M., Sogacheva, L., Aalto, P., Riipinen, I., Komppula, M. and co-authors. 2007. Aerosol size distribution measurements at four Nordic field stations: identification, analysis and trajectory analysis of new particle formation bursts. *Tellus* **59B**, 350–361.

Dockery, D. W. and Pope, C. A. III. 1994. Acute respiratory affects of particulate air pollution. *Ann. Rev. Public Health* **15**, 107–132.

Draxler, R. R. and Rolph, G. D. 2003. HYSPLIT (HYbrid Single-Particle Lagrangian Integrated Trajectory) Model access via NOAA ARL READY.NOAA Air Resources Laboratory, Silver Spring, MD. Available at http://www.arl.noaa.gov/ready/hysplit4.html.

Hakola, H., Rinne, J. and Laurila, T. 1998. The hydrocarbon emission rates of tea-leafed willow (Salix phylicifolia), silver birch (Betula pendula) and European aspen (Populus tremula). *Atmos. Environ.* **32**, 1825–1833.

Hellén, H., Hakola, H., Pystynen, K.-H., Rinne, J. and Haapanala, S. 2005. C2-C10 hydrocarbon emissions from a boreal wetland and forest floor. *Biogeosci. Discuss.* **2**, 1795–1814.

Hussein, T., Dal Maso, M., Petaja, T., Koponen, I. K., Paatero, P. and co-authors. 2005. Evaluation of an automatic algorithm for fitting the particle number size distributions. *Boreal Environ. Res.* **10**, 337–355.

Hyvärinen, A.-P., Komppula, M., Engler, C., Kivikäs, N., Kerminen, V. M. and co-authors. 2008. Atmospheric new particle formation at Utö, Baltic Sea 2003–2005. *Tellus* **60B**, doi:10.1111/j.1600-0889.2008.00343.x.

IPCC 2007. *Climate Change 2007 – The Physical Science Basi: Contribution of Working Group I to the Fourth Assessment Report of the IPCC*. Cambridge University Press, Cambridge, UK.

Janson, R. and De Serves, C. 1998. Isoprene emissions from boreal wetlands in Scandinavia. *J. Geophys. Res.* **103**, 25 513–25 517.

Kanakidou, M., Tsigaridis, K., Dentener, F. J. and Crutzen, P. J. 2000. Human-activity-enhanced formation of organic aerosols by biogenic hydrocarbon oxidation. *J. Geophys. Res.* **105**, 9243–9254.

Kavouras, I. G., Mihalopoulos, N. and Stephanou, E. G. 1998. Formation of atmospheric particles from organic acids produced by forests. *Nature* **395**, 683–686.

Komppula, M., Vana, M., Kerminen, V. M., Lihavainen, H., Viisanen, Y. and co-authors. 2007. Size distributions of atmospheric ions in the Baltic region. *Boreal Environ. Res.* **12**, 323–336.

Kristensson, A., Dal Maso, M., Swietlicki, E., Hussein, T., Zhou, J. and co-authors. 2008. Characterization of new particle formation events at a background site in southern Sweden: relation to air mass history. *Tellus* **60B**, doi:10.1111/j.1600-0889.2008.00345.x.

Kulmala, M. 2003. How particles nucleate and grow. *Science* **302**, 1000–1001.

Kulmala, M., Pirjola, L. and Mäkelä, J. M. 2000. Stable sulphate clusters as a source of new atmospheric particles. *Nature* **404**, 66–69.

Kulmala, M., Dal Maso, M., Makela, J. M., Pirjola, L., Vakeva, M. and co-authors. 2001. On the formation, growth and composition of nucleation mode particles. *Tellus B* **53**, 479–490.

Kulmala, M., Laakso, L., Lehtinen, K. E. J., Riipinen, I., Dal Maso, M. and co-authors. 2004a. Initial steps of aerosol growth. *Atmos. Chem. Phys.* **4**, 2553–2560.

Kulmala, M., Suni, T., Lehtinen, K. E. J., Dal Maso, M., Boy, M. and co-authors. 2004b. A new feedback mechanism linking forests, aerosols, and climate. *Atmos. Chem. Phys.* **4**, 557–562.

Kulmala, M., Vehkamäki, H., Petäjä, T., Dal Maso, M., Lauri, A. and co-authors. 2004c. Formation and growth rates of ultrafine atmospheric particles: a review of observations. *J. Aerosol Sci.* **35**, 143–176.

Kulmala, M., Lehtinen, K. E. J., Laakso, L., Mordas, G. and Hameri, K. 2005a. On the existence of neutral atmospheric clusters. *Boreal Environ. Res.* **10**, 79–87.

Kulmala, M., Petaja, T., Mönkkönen, P., Koponen, I. K., Dal Maso, M. and co-authors. 2005b. On the growh of nucleation mode particles: source rates of condensable vapor in polluted and clean environments. *Atmos. Chem. Phys.* **5**, 409–416.

Kulmala, M., Riipinen, I., Sipila, M., Manninen, H. E., Petaja, T. and co-authors. 2007. Towards direct measurement of atmospheric nucleation. *Science (Express Reports)*, doi:10.1126/science.1144124.

Laakso, L., Petäjä, T., Lehtinen, K. E. J., Kulmala, M., Paatero, J. and co-authors. 2004. Ion production rate in aboreal forest based on ion, particle and radiation measurements. *Atmos. Chem. Phys.* **4**, 1933–1943.

Mäkelä, J. M., Yli-Koivisto, S., Hiltunen, V., Seidl, W., Swietlicki, E. and co-authors. 2001. Chemical composition of aerosol during particle formation events in boreal forest. *Tellus* **53B**, 380–393.

Mirme, A., Tamm, E., Mordas, G., Vana, M., Uin, J. and co-authors. 2007. A wide-range multi-channel air ion spectrometer. *Boreal Environ. Res.* **12**, 247–264.

Nilsson, E. D., Rannik, U., Kulmala, M., Buzorius, G. and O'Dowd, C. D. 2001. Effects of continental boundary layer evolution, convection, turbulence and entrainment, on aerosol formation. *Tellus* **53B**, 441–461.

O'Dowd, C., Aalto, P., Hämeri, K., Kulmala, M. and Hoffmann, T. 2002. Atmospheric particles from organic vapours. *Nature* **416**, 497–498.

O'Dowd, C. D., Facchini, M. C., Cavalli, F., Ceburnis, D., Mircea, M. and co-authors. 2004. Biogenically driven organic contribution to marine aerosol. *Nature* **431**, 676–680.

Pope, C. A., III, Burnett, R. T., Thun, M. J., Calle, E. E., Krewski, D. and co-authors. 2002. Lung cancer, cardiopulmonary mortality, long-term exposure to fine particlate air pollution. *J. Am. Med. Assoc.* **287**, 1132–1141.

Riipinen, I., Sihto, S.-L., Kulmala, M., Arnold, F., Dal Maso, M. and co-authors. 2007. Connections between atmospheric sulphuric acid and new particle fomration during QUEST III-IV campaigns in Heidelberg and Hyytiälä. *Atmos. Chem. Phys.* **7,** 1899–1914.

Rolph, G. D. 2003. Real-time environmental applications and display system (READY). NOAA Air Resources Laboratory, Silver Spring, MD. Available at http://www.arl.noaa.gov/ready/hysplit4.html.

Sihto, S.-L., Kulmala, M., Kerminen, V. M., Dal Maso, M., Petaja, T. and co-authors. 2006. Atmospheric sulphuric acid and aerosol formation: implications from atmospheric measurements for nucleation and early growth mechanisms. *Atmos. Chem. Phys.* **6**, 4079–4091.

Spracklen, D. V., Carslaw, K. S., Kulmala, M., Kerminen, V. M., Mann, G. W. and co-authors. 2006. The contribution of boundary layer nucleation events to total particle concentrations on regional and globl scales. *Atmos. Chem. Phys.* **6**, 5631–5648.

Suni, T., Kulmala, M., Hirsikko, A., Bergman, T., Laakso, L. and co-authors. 2007. Formation and characteristics of ions and charged aerosol particles in a native Australian Eucalypt forest. *Atmos. Chem. Phys. (Discussion)* **7**, 10 343–10 369.

Svensson, B. H., Christensen, T. R., Johansson, E. and Öquist, M. 1999. Interdecadal variations in CO_2 and CH_4 exchange of a subarctic mire – Stordalen revisited after 20 years. *Oikos* **85(1)**, 22–30.

Tammet, H. 1995. Size and mobility of nanometer particles, clusters, and ions. *J. Aerosol Sci.* **26**, 459–475.

Tammet, H. 2006. Continuous scanning of the mobility and size distribution of charged cluster and nanometer particles in atmospheric air and the balanced scanning mobility analyzer BSMA. *Atmos. Res.* **82**, 523–535.

Tunved, P., Hansson, H. C., Kerminen, V. M., Ström, J., Dal Maso, M. and co-authors. 2006. High natural aerosol loading over boreal forests. *Science* **312**, 261–263.

Vartiainen, E., Kulmala, M., Ehn, M., Hirsikkko, A., Junninen, H. and co-authors. 2007. Ion and particle number concentrations and size distributions along the Trans-Siberian railroad. *Boreal Environ. Res.* **12**, 375–396.

Venzac, H., Sellegri, K. and Laj, P. 2007. Nucleation events detected at the high altitude site of the Puy de Dôme Research Station, France. *Boreal Environ. Res.* **12**, 345–360.

Weber, R. J., Eisele, F. L., Marti, J. J., Tanner, T. and Jefferson, A. 1996. Measured atmospheric new particle formation rates: implications for nucleation mechanisms. *Chem. Eng. Commun.* **151**, 53–64.